



The Unsteady Aerodynamics Module for FAST 8

Rick Damiani and Greg Hayman

National Renewable Energy Laboratory

**NREL is a national laboratory of the U.S. Department of Energy
Office of Energy Efficiency & Renewable Energy
Operated by the Alliance for Sustainable Energy, LLC**

This report is available at no cost from the National Renewable Energy Laboratory (NREL) at www.nrel.gov/publications.

Contract No. DE-AC36-08GO28308

Technical Report
NREL/TP-5000-66347
November 2019



The Unsteady Aerodynamics Module for FAST 8

Rick Damiani and Greg Hayman

National Renewable Energy Laboratory

Suggested Citation

Damiani, Rick, and Greg Hayman. 2019. *The Unsteady Aerodynamics Module for FAST 8*. Golden, CO: National Renewable Energy Laboratory. NREL/TP-5000-66347.
<https://www.nrel.gov/docs/fy20osti/66347.pdf>.

**NREL is a national laboratory of the U.S. Department of Energy
Office of Energy Efficiency & Renewable Energy
Operated by the Alliance for Sustainable Energy, LLC**

This report is available at no cost from the National Renewable Energy Laboratory (NREL) at www.nrel.gov/publications.

Contract No. DE-AC36-08GO28308

Technical Report
NREL/TP-5000-66347
November 2019

National Renewable Energy Laboratory
15013 Denver West Parkway
Golden, CO 80401
303-275-3000 • www.nrel.gov

NOTICE

This work was authored by the National Renewable Energy Laboratory, operated by Alliance for Sustainable Energy, LLC, for the U.S. Department of Energy (DOE) under Contract No. DE-AC36-08GO28308. Funding provided by the U.S. Department of Energy Office of Energy Efficiency and Renewable Energy Wind Energy Technologies Office. The views expressed herein do not necessarily represent the views of the DOE or the U.S. Government.

This report is available at no cost from the National Renewable Energy Laboratory (NREL) at www.nrel.gov/publications.

U.S. Department of Energy (DOE) reports produced after 1991 and a growing number of pre-1991 documents are available free via www.OSTI.gov.

Cover Photos by Dennis Schroeder: (clockwise, left to right) NREL 51934, NREL 45897, NREL 42160, NREL 45891, NREL 48097, NREL 46526.

NREL prints on paper that contains recycled content.

Executive Summary

The new modularization framework of FAST v.8 (Jonkman 2013) was accompanied by a complete overhaul of the aerodynamics routines. AeroDyn is an aerodynamics module comprised of four submodels: rotor wake/induction, blade airfoil aerodynamics, tower influence on the blade nodes, and tower drag. Throughout the software overhaul, several improvements to the original theoretical treatments were achieved, including more accurate skewed-wake and unsteady airfoil aerodynamics, and the possibility of modeling highly flexible and curved blades.

Under asymmetric conditions, such as wind shear, yawed, and tilted flow, the individual blade elements undergo variations in angle of attack that lead to unsteady aerodynamics phenomena, which can no longer be captured through the static airfoil lift and drag look-up tables. This document covers the main theory and the organization of the modularization framework of the new unsteady aerodynamics submodule (UAM)¹, which includes unsteady aerodynamics under attached flow conditions and dynamic stall. The UAM can be called by either blade element momentum theory (only interface discussed in this report), or other future wake models (e.g., dynamic blade element momentum theory, or generalized dynamic wake).

¹UAM is a submodule to OpenFAST's aerodynamics module (AeroDyn), but we will continue using the term module for simplicity.

Acknowledgments

This document was reviewed and improved thanks to the input provided by Michael Sprague, Jason Jonkman, and Bonnie Jonkman.

Table of Contents

List of Acronyms	2
List of Symbols	2
List of Subscripts and Superscripts	8
List of Greek Symbols	8
1 Overview	11
1.1 Unsteady Attached Flow and Its Indicial Treatment	12
1.1.1 Normal Force	14
1.1.2 Chordwise Force	17
1.1.3 Pitching Moment	18
1.2 TE Flow Separation	19
1.2.1 Normal Force	20
1.2.2 Chordwise Force	21
1.2.3 Pitching Moment	21
1.3 Dynamic Stall	22
1.3.1 Normal Force	22
1.3.2 Chordwise Force	23
1.3.3 Pitching Moment	23
2 Inputs, Outputs, Parameters, States, and Implementation of UA	24
2.1 Init_Inputs	24
2.2 Inputs u	25
2.3 Outputs y	25
2.4 States x_d	25
2.5 Parameters p	26
2.6 UA Implementation	27
2.6.1 UA_Init Routine	27
2.6.2 UA_UpdateStates Routine	27
2.6.2.1 UAmod Logical Flags	27
2.6.2.2 Update Discrete States	28
2.6.2.3 Update Other States	29
2.6.2.3.1 T_f modifications	29
2.6.2.3.2 T_V modifications	29
2.6.2.3.3 Update ‘previous time step’ states	30
2.6.3 UA_CalcOutput	30
Bibliography	31

List of Figures

Figure 1.	Conventional stages of dynamic stall (Leishman 2006)	12
Figure 2.	Conventional stages of dynamic stall and associated C_l , C_d , and C_m as functions of angle of attack (AOA) from Leishman (2006)	13
Figure 3.	Main definitions of blade element (BE) forces (denoted via their normalized coefficients) for the unsteady aerodynamics (UA) treatment (Damiani 2011)	14
Figure 4.	Block diagram showing the order of the calls to the subroutines (AeroDyn_CalcOutput happens first, AeroDyn_UpdateStates happens second) and the overall organization from the parent module AeroDyn to UA	24

List of Acronyms

2D	two-dimensional
3D	three-dimensional
AeroDyn	OpenFAST's aerodynamics module
AOA	angle of attack
AOI	angle of incidence
BE	blade element
BEMT	blade element momentum theory
DBEMT	dynamic blade element momentum theory
DS	dynamic stall
GDW	generalized dynamic wake
LBM	Leishman-Beddoes model
LE	leading edge
MT	momentum theory
TE	trailing edge
UA	unsteady aerodynamics
UAM	unsteady aerodynamics submodule

List of Symbols

AFI_{params}	Airfoil static tables of C_l , C_d , C_m , and UA parameters
----------------	--

A_1	Constant in the expression of ϕ_α^c and ϕ_q^c ; experimental results (Leishman 2011) set it equal to 0.3; this value is relatively insensitive for thin airfoils but may be different for turbine airfoils; generally speaking, it should not be tuned by the user
A_2	Constant in the expression of ϕ_α^c and ϕ_q^c ; experimental results (Leishman 2011) set it to 0.7; this value is relatively insensitive for thin airfoils but may be different for turbine airfoils; generally speaking, it should not be tuned by the user
A_5	Constant in the expression of K_q''' , $C_{m_q}^{nc}(s, M)$, and $k_{m,q}(M)$; experimental results (Leishman 2006) set it equal to 1
C_{LP}	Low-pass-filter constant
D	Rotor diameter
$F_R(s)$	Response function to generic disturbance $\varepsilon(s)$
$F_R(t)$	Response function to generic disturbance $\varepsilon(t)$
<i>FirstPass</i>	Flag indicating first time step
<i>LESF</i>	Leading-edge separation flag
M	Mach number
<i>NumBlades</i>	Number of blades
<i>NumOuts</i>	Number of output channels
R	Rotor radius
S_1	Constant in the f curve best-fit for $\alpha_0 \leq \alpha \leq \alpha_1$; by definition it depends on the airfoil
S_2	Constant in the f curve best-fit for $\alpha > \alpha_1$; by definition it depends on the airfoil
S_3	Constant in the f curve best-fit $\alpha_2 \leq \alpha < \alpha_0$; by definition it depends on the airfoil
S_4	Constant in the f curve best-fit for $\alpha < \alpha_2$; by definition it depends on the airfoil
St_{sh}	Strouhal's shedding frequency constant, commonly taken equal to 0.19
T'_α	Mach-dependent, nondimensional time constant in the expression of ϕ_α^{nc}
T'_q	Mach-dependent, nondimensional time constant in the expression of ϕ_q^{nc}
<i>TESF</i>	Trailing-edge separation flag
T_I	Time constant in the expression of $\phi_\alpha^{nc} = c/a_s$
T_V	Time constant associated with the vortex lift decay process; it is used in the expression of C_n^v . It depends on Re , M , and airfoil type
$T_\alpha(M)$	Mach-dependent time constant in the expression of ϕ_α^{nc}
T_f	Constant dependent on Mach, Re , and airfoil shape; it is used in the expression of D_f and f''
T_p	Boundary-layer, LE pressure gradient time constant in the expression of D_p , which should be tuned based on airfoil experimental data
$T_q(M)$	Mach-dependent time constant in the expression of ϕ_q^{nc}

T_{V0}	Initial value of T_V
T_{VL}	Time constant associated with the vortex advection process; it represents the nondimensional time in semichords needed for a vortex to travel from LE to TE; it is used in the expression of C_n^v ; it depends on Re , M (weakly), and airfoil. Value's range = [6; 13]
T_{f0}	Initial value of T_f
$T'_{m,q}$	Mach-dependent time constant in the expression of $\phi_{m,q}^{nc}$
$T_{m,q}(M)$	Mach-dependent time constant in the expression of $\phi_{m,q}^{nc}$
T_{sh}	Time constant associated with the vortex shedding; it allows multiple vortices to be shed at a Strouhal's frequency of 0.19
$UAmod$	Switch to select handling of options and possible methods in the UA treatment
$VRTX$	Vortex advection flag
X_1	Deficiency function used in the development of $C_{n\alpha}^c(s, M)$
X_2	Deficiency function used in the development of $C_{n\alpha}^c(s, M)$
X_3	Deficiency function used in the development of $C_{nq}^c(s, M)$
X_4	Deficiency function used in the development of $C_{nq}^c(s, M)$
\bar{x}_{cp}	Constant in the expression of \hat{x}_{cp}^v , usually equal to 0.2
$K_{\alpha LP, -1}$	Previous time-step value of low-pass-filtered K_α
$K_{q LP, -1}$	Previous time-step value of low-pass-filtered K_q
$\alpha_{, -1}$	Previous time-step value of α
f_m''	CENER's proposed version of lagged f_m'
f_m'	CENER's proposed lookup version of f'
$f'', -1$	Previous time-step value of f''
$f', -1$	Previous time-step value of f'
$q, -1$	Previous time-step value of q
$q_{LP, -1}$	Previous time-step value of low-pass-filtered q
\hat{k}_1	Constant in the C_c expression due to LE vortex effects
\hat{k}_2	Constant in the C_c expression due to leading edge (LE) vortex effects, taken equal to $2(C_n' - C_{n1}) + (f'' - f)$
\hat{x}_{AC}	Aerodynamic center distance from LE in percent chord
\hat{x}_{cp}^v	Center-of-pressure distance from the $1/4$ -chord, in percent chord, during the LE vortex advection process
\hat{x}_{cp}	Center-of-pressure distance from LE in percent chord
a_s	Speed of sound

b_1	Constant in the expression of ϕ_α^c and ϕ_q^c ; experimental results (Leishman 2011) set it equal to 0.14; this value is relatively insensitive for thin airfoils but may be different for turbine airfoils; generally speaking, it should not be tuned by the user
b_2	Constant in the expression of ϕ_α^c and ϕ_q^c ; experimental results (Leishman 2011) set it equal to 0.53. This value is relatively insensitive for thin airfoils but may be different for turbine airfoils; generally speaking, it should not be tuned by the user
b_5	Constant in the expression of K_q''' , $C_{m_q}^{nc}(s, M)$, and $k_{m,q}(M)$; experimental results (Leishman 2006) set it equal to 5
f_c''	Lagged version of f_c'
$f_{c,-1}''$	Previous time-step value of f_c''
f_c'	f' calculated from Kirchhoff's expression containing C_c function of f
f_n'	f' calculated from Kirchhoff's expression containing C_n function of f
$f_{c,-1}'$	Previous time-step value of f_c'
$flookup$	Logical flag to indicate whether a lookup (True) or an interpolation of the airfoil data tables (False) is used to retrieve the values for f
$iBlade$	Blade index
$jBladeNode$	Blade node index
k_0	Constant in the \hat{x}_{cp} curve best-fit; $= (\hat{x}_{AC} - 0.25)$
k_1	Constant in the \hat{x}_{cp} curve best-fit
k_2	Constant in the \hat{x}_{cp} curve best-fit
k_3	Constant in the \hat{x}_{cp} curve best-fit
$k_\alpha(M)$	Mach-dependent constant in the expression of $T_\alpha(M)$
$k_q(M)$	Mach-dependent constant in the expression of $T_q(M)$
$k_{m,q}(M)$	Mach-dependent constant in the expression of $T_{m,q}(M)$ and $C_{m_q}^{nc}(s, M)$
$miscVars$	Other local variables (not saved between calls to <i>UpdateStates</i> and <i>CalcOutputs</i> and when backing up in time)
$nNodesPerBlade$	Number of nodes per blade
q	Nondimensional pitching rate $= \dot{\alpha}c/U$
s	Nondimensional distance
t	Time
x_d	Discrete states
$D_{\alpha f,-1}$	Previous time-step value of $D_{\alpha f}$
$D_{f,-1}$	Previous time-step value of D_f
$D_{p,-1}$	Previous time-step value of D_p
$K'_{\alpha,-1}$	Previous time-step value of K'_α
$K_{\alpha LP}$	Modified value of K_α due to filtered α and q
$K'''_{q,-1}$	Previous time-step value of K'''_q
$K''_{q,-1}$	Previous time-step value of K''_q

$K'_{q,-1}$	Previous time-step value of K'_q
K_{qLPn-1}	Low-pass-filtered value of K_q at the (n-1)-th time step
K_{qLP}	Low-pass-filtered value of K_q
$X_{1,-1}$	Previous time-step value of X_1
$X_{2,-1}$	Previous time-step value of X_2
$X_{3,-1}$	Previous time-step value of X_3
$X_{4,-1}$	Previous time-step value of X_4
$C_n^{pot,-1}$	Previous time-step value of C_n^{pot}
$C_n^v,-1$	Previous time-step value of C_n^v
$C_{V,-1}$	Previous time-step value of C_V
q_{LPn-1}	Value of q_{LP} at the (n-1)-th time step
q_{n-1}	Value of q at the (n-1)-th time step
c	Chord length
C_c	2D tangential (along chord) force coefficient
C_c^{fs}	2D tangential (along chord) force coefficient under TE flow separation conditions
C_c^{pot}	2D along-chord force coefficient under attached (potential) flow conditions
C_d	2D drag coefficient
C_{d0}	2D drag coefficient at 0-lift
C_l	2D lift coefficient
$C_{l\alpha}$	Slope of the 2D lift coefficient curve
C_m	2D pitching moment coefficient about 1/4-chord; positive if nose up
C_{m0}	2D pitching moment coefficient at 0-lift, positive if nose up
$C_{m\alpha}(s, M)$	Pitching moment coefficient response to step change in α
$C_{m\alpha}^c(s, M)$	Circulatory component of the pitching moment coefficient response to step change in α
$C_{m\alpha}^{nc}(s, M)$	Noncirculatory component of the pitching moment coefficient response to step change in α
$C_{m\alpha,q}(s, M)$	Moment coefficient response to step change in α and q
$C_{m\alpha,q}^c(s, M)$	Circulatory component of $C_{m\alpha,q}(s, M)$
$C_{m\alpha,q}^{nc}(s, M)$	Noncirculatory component of $C_{m\alpha,q}(s, M)$
$C_{m_q}(s, M)$	Pitching moment coefficient response to step change in q
$C_{m_q}^c(s, M)$	Circulatory component of the pitching moment coefficient response to step change in q
$C_{m_q}^{nc}(s, M)$	Noncirculatory component of the moment coefficient response to step change in q
$C_{m\alpha}$	Slope of the 2D pitching moment coefficient curve
C_m^{fs}	2D tangential 1/4-chord pitching moment coefficient under TE flow separation conditions.
C_m^{pot}	2D moment coefficient under attached (potential) flow conditions about 1/4-chord location

$C_{mq}(s, M)$	Slope of the pitching moment coefficient versus q curve
C_m^v	Pitching moment coefficient due to the presence of LE vortex
C_n	2D normal-to-chord force coefficient
C_{n1}	Critical value of C'_n at LE separation. It should be extracted from airfoil data at a given Mach and Reynolds number. It can be calculated from the static value of C_n at either the break in the pitching moment or the loss of chord force at the onset of stall. It is close to the condition of maximum lift of the airfoil at low Mach numbers.
C_{n2}	Critical value of C'_n at LE separation for negative AOAs; analogous to C_{n1}
$C_{n\alpha}(s, M)$	Normal force coefficient response to step change in α
$C_{n\alpha}^c(s, M)$	Circulatory component of the normal force coefficient response to step change in α
$C_{n\alpha}^{nc}(s, M)$	Noncirculatory component of the normal force coefficient response to step change in α
$C_{n\alpha,q}(s, M)$	Normal force coefficient response to step change in α and q
$C_{n\alpha,q}^c(s, M)$	Circulatory component of $C_{n\alpha,q}(s, M)$
$C_{n\alpha,q}^{nc}(s, M)$	Noncirculatory component of $C_{n\alpha,q}(s, M)$
$C_n^c(s, M)$	Circulatory component of $C_n(s, M)$
$C_n^c(s, M)$	Normal force coefficient response to step change in q
$C_{nq}^c(s, M)$	Circulatory component of the normal force coefficient response to step change in q
$C_{nq}^{nc}(s, M)$	Noncirculatory component of the normal force coefficient response to step change in q
$C_{n\alpha}(M)$	Slope of the 2D normal coefficient curve, similar to $C_{l\alpha}$
$C_{n\alpha}^c(s, M)$	Slope of the circulatory normal force coefficient versus α curve
C_n^{fs}	Normal force coefficient under TE flow separation conditions
C_n'	Lagged component of C_n in the trailing edge (TE) separated treatment
C_n^{pot}	2D normal-to-chord force coefficient under attached (potential) flow conditions
$C_n^{pot,c}$	Circulatory part of 2D normal-to-chord force coefficient under attached (potential) flow conditions
$C_n^{pot,nc}$	Noncirculatory part of 2D normal-to-chord force coefficient under attached (potential) flow conditions
$C_{nq}(s, M)$	Slope of the normal force coefficient versus q curve
C_n^v	Normal force coefficient due to the presence of LE vortex

C_V	Contribution to the normal force coefficient due to accumulated vorticity in the LE vortex
D_{α_f}	Deficiency function for α_f
D_f	Deficiency function for f'
$D_{f_c, -1}$	Previous time-step value of D_{f_c}
D_{f_c}	Deficiency function for f'_c
D_p	Deficiency function for C'_n
f	Separation point distance from LE in percent chord
f_m	CENER's proposed version of f extracted from the C_m static tables, assuming $C_m = C_n f_m$
f'_m	Version of f_m extracted from the airfoil C_m static tables with α_f as input parameter
f''_m	Lagged version of f'_m
f'	Separation point distance from LE in percent chord under unsteady conditions
f''	Lagged version of f' accounting for unsteady boundary layer response
k	Reduced frequency
K_α	Backward finite difference of α
K'_α	Deficiency function for $C^{nc}_{n\alpha}(s, M)$
K_q	Backward finite difference of q
K'_q	Deficiency function for $C^{nc}_{nq}(s, M)$
K''_q	Deficiency function for $C^{nc}_{mq}(s, M)$
K'''_q	Deficiency function for $C^c_{mq}(s, M)$
Re	Airfoil-chord Reynolds number
U	Air velocity magnitude relative to the airfoil
U_{inf}	Freestream air velocity magnitude

List of Subscripts and Superscripts

c	Circulatory component of the quantity at the base
nc	Noncirculatory component of the quantity at the base
α	Relative to a step change in α
n	relative to the n-th time step
q	Relative to a step change in q
t	Relative to the n-th time step

List of Greek Symbols

$\Delta\alpha_0$	$\alpha - \alpha_0$
$\alpha_{LP, -1}$	Previous time-step value of low-pass-filtered α
α_{LP_n}	Low-pass-filtered value of α
$\alpha_{LP_{n-1}}$	Low-pass-filtered value of α at the (n-1)-th time step
$\epsilon(s)$	Generic disturbance function of s

$\varepsilon(t)$	Generic disturbance function of t
η_e	Recovery factor $\simeq [0.85 - 0.95]$ to account for viscous effects at limited or no separation on C_c
$\tau_{V,-1}$	Previous time-step value of τ_V
ω	Generic frequency
$\phi(s, M)$	Indicial response function
$\phi(t, M)$	Indicial response function
ϕ_α^c	Normal force coefficient, circulatory indicial response function to a step change in α
ϕ_α^{nc}	Normal force coefficient, noncirculatory indicial response function to a step change in α
ϕ_q^c	Normal force coefficient, circulatory indicial response function to a step change in q
ϕ_q^{nc}	Normal force coefficient, noncirculatory indicial response function to a step change in q
$\phi_{m,\alpha}^{nc}$	Pitching moment coefficient, noncirculatory indicial response function to a step change in α
$\phi_{m,q}^c$	Pitching moment coefficient, circulatory indicial response function to a step change in q
$\phi_{m,q}^{nc}$	Pitching moment coefficient, noncirculatory indicial response function to a step change in q
σ_1	Generic multiplier for T_f
σ_3	Generic multiplier for T_V
σ_s	Generic integrand coordinate
σ_t	Generic integrand coordinate
τ_V	Time variable that tracks the travel of the LE vortex over the airfoil suction surface. It is made dimensionless via the semichord: $\tau_V = t * 2U/c$. If less than $2T_{VL}$, it renders the logical flag $VRTX=True$; if less than T_{VL} , then the vortex is still on the airfoil
ζ_{LP}	Low-pass-filter frequency cutoff (-3 dB)
q_{LP}	Low-pass-filtered value of q
α	Angle of attack
α_0	0-lift angle of attack
α_1	Angle of attack at $f=0.7$ (approximately the stall angle), for $\alpha \geq \alpha_0$
α_2	Angle of attack at $f=0.7$ for $\alpha < \alpha_0$
α_f	Effective AOI that would give the same unsteady LE pressure gradient under static conditions; used to calculate f'
α_e	Effective angle of attack at $3/4$ -chord
α'_f	Lagged version of α_f ; used in Minnema's (1998) calculation of C_m under separated conditions
α_n	Value of α at the n -th time step, i.e., $t = n\Delta t$
$\alpha_{f,-1}$	Previous time-step value of α_f
α_{n-1}	Value of α at the $(n-1)$ -th time step, i.e., $t = (n - 1)\Delta t$
β_M	Prandtl-Glauert compressibility correction factor $\sqrt{1 - M^2}$

Δs Incremental variation in s for the Δt time step
 Δt Time step

1 Overview

Because of turbulence, wind shear, control inputs, and off-axis operations, wind turbine rotors experience unsteady aerodynamic loading. Unsteady aerodynamics are primarily caused by two physical mechanisms. First, the unsteady (indicial) variation in the two-dimensional (2D) lift, drag, and moment coefficient associated with an unsteady variation of the angle of attack, wherein the timescale is on the order of tenths of seconds, or $\sim c/\omega R$ with c representing the chord length, ω the generic frequency, and R the rotor radius. Second, induction effects driven by the midwake region with a time constant of a few seconds, or $\sim D/U_{\text{inf}}$, with D as the rotor diameter and U_{inf} as the freestream air velocity magnitude. The first mechanism pertains to the near-wake field, which affects the BE portion of the blade element momentum theory (BEMT), and is the focus of this manual. The second mechanism is affected by the dynamics of the vorticity shed in the midwake and affects the momentum theory (MT) portion of the BEMT (Damiani, 2016, forthcoming). In this document, UA refers to unsteady aerodynamics, or the first physical mechanism.

The main theory follows the work by Leishman and Beddoes (1986, 1989), Pierce and Hansen (1995), Pierce (1996), Leishman (2011), and Damiani (2011). UA is driven mostly by 2D flow aspects, including that of dynamic stall (DS). DS is a well-known phenomenon that can affect wind turbine performance and loading, especially during yawed operations, and can result in large unsteady stresses on the structures. DS manifests as a delay in the onset of flow separation to higher angles of attack (AOAs) that would otherwise occur under static (steady) conditions, followed by an abrupt flow separation from the leading edge (LE) of the airfoil (Leishman 2011). The LE separation is the fundamental characteristic of the DS of an airfoil; in contrast, quasi-steady stall would start from the airfoil trailing edge (TE).

DS occurs for reduced frequencies (k) above 0.02, where:

$$k = \frac{\omega c}{2U} \quad (1.1)$$

The five stages of DS are as follows and shown in Figure 1 and Figure 2:

1. Onset of flow reversal
2. Flow separation and vorticity accumulation at the LE
3. Shedding of the vortex and convection along the suction surface of the airfoil (lift increases)
4. Lift stall (vortex is shed in the wake and lift, causing an abrupt drop off)
5. Reattachment of the flow at AOAs considerably lower than static AOAs (hysteresis).

The model chosen to represent UA and DS is the Leishman-Beddoes model (LBM) because it is the most widely used, has the most support throughout the community, and has shown reasonable success when compared to experimental data. The LBM is a postdictive model and as such it will not solve equations of motion, though the principles are fully rooted in the physics of unsteady flow.

In the LBM, the different processes are modeled as first-order subsystems with differential equations with predetermined constants to match experimental results. Therefore, *knowledge of the airfoil characteristics under UA is a prerogative* of the LBM. The LBM can also be described as an indicial response (i.e., response to a series of small disturbances) model for attached flow, extended to account for separated flow effects and vortex lift. Forces are computed as normal and tangential (to chord) and pitching moment about the 1/4-chord location (see also Figure 3 and Eq. (1.2)). Note that in Eq. (1.2), the total drag is explicitly given by the sum of pressure and viscous shear components.

$$\begin{aligned} C_l &= C_n \cos \alpha + C_c \sin \alpha \\ C_d &= C_n \sin \alpha - C_c \cos \alpha + C_{d0} \end{aligned} \quad (1.2)$$

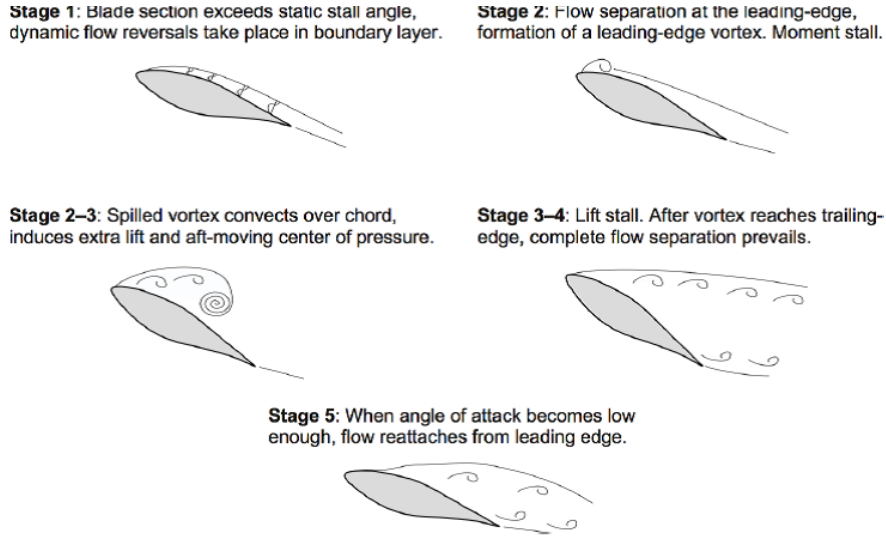


Figure 1. Conventional stages of dynamic stall (Leishman 2006)

$$\begin{aligned}
 C_n &= C_l \cos \alpha + (C_d - C_{d0}) \sin \alpha \\
 C_c &= C_l \sin \alpha - (C_d - C_{d0}) \cos \alpha
 \end{aligned}
 \tag{1.3}$$

The original model was developed for helicopters but has been successfully applied to wind turbines (see Pierce (1996) and Gupta and Leishman (2006)). Yawed flow conditions, Coriolis, and centrifugal forces that lead to three-dimensional (3D) effects were not included in the original model.

The LBM considers a number of UA conditions, including attached flow conditions and TE separation before stall, delays associated with the unsteady onset of DS and accompanying boundary layer development, advection of the LE vortex, shedding in the wake, and suppression of TE separation in favor of LE separation. The LBM can be divided into three main submodules:

1. Unsteady, attached flow solution via indicial treatment (potential flow)
2. TE flow separation
3. DS vorticity advection.

1.1 Unsteady Attached Flow and Its Indicial Treatment

The advantage of the indicial treatment is that a response to an arbitrary forcing can be obtained by superpositioning response functions to a step variation in AOA, pitch rate, or heave (plunging) motion. The superposition is carried out via the so-called Duhamel Integral (Leishman 2006), which for the generic response $F_R(t)$ to a generic disturbance $\varepsilon(t)$ can be written as:

$$\begin{aligned}
 F_R(t) &= \varepsilon(0)\phi(t, M) + \int_0^t \frac{d\varepsilon}{d\sigma_t}(\sigma_t)\phi(t - \sigma_t, M)d\sigma_t \\
 \text{or} & \\
 F_R(s) &= \varepsilon(0)\phi(s, M) + \int_0^s \frac{d\varepsilon}{d\sigma_s}(\sigma_s)\phi(s - \sigma_s, M)d\sigma_s
 \end{aligned}
 \tag{1.4}$$

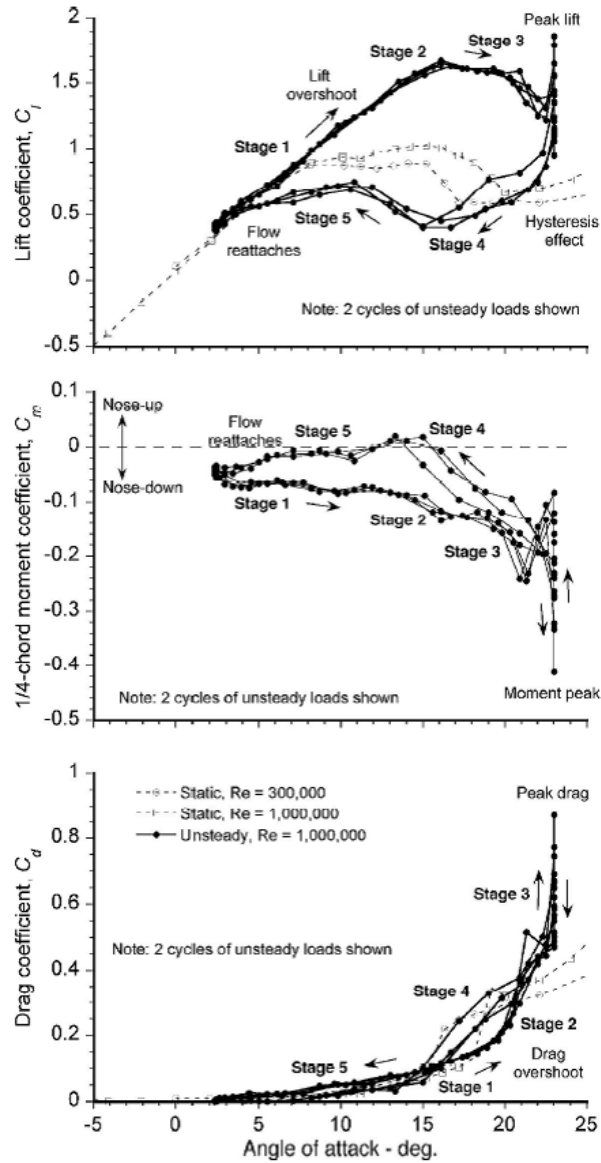


Figure 2. Conventional stages of dynamic stall and associated C_l , C_d , and C_m as functions of AOA from Leishman (2006)

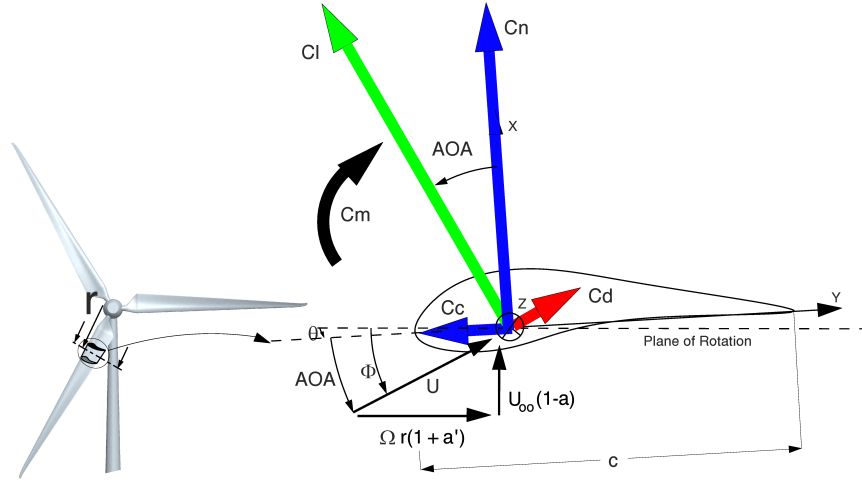


Figure 3. Main definitions of BE forces (denoted via their normalized coefficients) for the UA treatment (Damiani 2011)

where t is time, M is the Mach number, σ_t and σ_s are generic integrand coordinates, and s is the nondimensional distance, defined as:

$$s = \frac{2}{c} \int_0^t U(t) dt \quad (1.5a)$$

$$\Delta s = \frac{2}{c} U(t) \Delta t \quad (1.5b)$$

where the airfoil half chord ($c/2$) was taken as the nondimensionalizing factor, and U is the air velocity magnitude relative to the airfoil.

The indicial functions ($\phi(s, M)$) are surmised into two components: the first is related to the noncirculatory (superscript 'nc') loading (piston theory and acoustic wave theory), and the second (superscript 'c') originates from the development of circulation about the airfoil. The noncirculatory part depends not only on the instantaneous airfoil motion, but on the time history of the prior motion. The circulatory response can be calculated via the 'lumped approach', wherein the effects of step changes in AOA (α), pitch rate, heave motion, and so on are combined into an effective AOA at the $3/4$ -chord station.

1.1.1 Normal Force

The normal force coefficient response to a step change in nondimensional pitch rate q and a step change in AOA can be written as a function of the indicial functions as shown in Eq. (1.6):

$$\begin{aligned} C_{n_{\alpha,q}}(s, M) &= C_{n_{\alpha}}(s, M) + C_{n_q}(s, M) = C_{n_{\alpha}}(M)\alpha + C_{n_q}(s, M)q \\ C_{n_{\alpha}}(s, M) &= \frac{4}{M} \phi_{\alpha}^{nc} + \frac{C_{n_{\alpha}}(M)}{\beta_M} \phi_{\alpha}^c \\ C_{n_q}(s, M) &= \frac{1}{M} \phi_q^{nc} + \frac{C_{n_{\alpha}}(M)}{2\beta_M} \phi_q^c \end{aligned} \quad (1.6)$$

where β_M is the Prandtl-Glauert compressibility correction factor $\sqrt{1-M^2}$, and $C_{n_{\alpha}}(M)$ is the slope of the 2D normal coefficient curve, similar to $C_{l_{\alpha}}$.

The nondimensional pitch rate q is given by:

$$q = \frac{\dot{\alpha}c}{U} \simeq \frac{K_{\alpha_n}c}{U} \quad (1.7)$$

with : $K_{\alpha_n} = \frac{\alpha_n - \alpha_{n-1}}{\Delta t}$

where the subscript ‘n’ denotes the n-th time step.

For small Δt 's, the finite difference K_{α} can be subjected to significant numerical noise. To smooth out the terms associated with time derivatives, a low-pass-filter is introduced. The filter is applied to α , q , and its derivative K_q (which is used later) as defined in Eq. (1.8):

$$\begin{aligned} \alpha_{LPn} &= C_{LP}\alpha_{LPn-1} + (1 - C_{LP})\alpha_n \\ q_n &= \frac{(\alpha_{LPn} - \alpha_{LPn-1})c}{U_n\Delta t} \\ q_{LPn} &= C_{LP}q_{LPn-1} + (1 - C_{LP})q_n \\ K_{\alpha LPn} &= \frac{q_{LPn}U_n}{c} \\ K_{qn} &= \frac{q_n - q_{n-1}}{\Delta t} \\ K_{qLPn} &= C_{LP}K_{qLPn-1} + (1 - C_{LP})K_{qn} \end{aligned} \quad (1.8)$$

with :

$$C_{LP} = e^{-2\pi\Delta t\zeta_{LP}}$$

and where α_{LPn} is the low-pass-filtered value of α , q_{LP} is the low-pass-filtered value of q , $K_{\alpha LP}$ is the modified value of K_{α} due to filtered α and q , K_q is the backward finite difference of q , K_{qLP} is the low-pass-filtered value of K_q , C_{LP} is the low-pass-filter constant, and ζ_{LP} is the low-pass-filter frequency cutoff (-3 dB).

From here on, the ‘LP’ subscript is dropped with the understanding that quantities such as α , K_{α} , q , and K_q denote the respective filtered quantities α_{LPn} , $K_{\alpha LP}$, q_{LP} , and K_{qLP} as defined in Eq. (1.8).

The indicial responses can then be approximated as in Eq. (1.9) (Leishman and Beddoes 1989; Johansen 1999):

$$\begin{aligned} \phi_{\alpha}^c &= \phi_q^c = 1 - A_1 \exp(-b_1\beta_M^2 s) - A_2 \exp(-b_2\beta_M^2 s) \\ \phi_{\alpha}^{nc} &= \exp\left(-\frac{s}{T'_{\alpha}}\right) \\ \phi_q^{nc} &= \exp\left(-\frac{s}{T'_q}\right) \end{aligned} \quad (1.9)$$

where A_1 , A_2 , b_1 , and b_2 are constants that were tuned from experimental results on oscillating airfoils in the wind tunnel, and that are relatively insensitive to the airfoil shapes, at least for thin airfoils such as those used in rotorcraft (see ‘List of Symbols’ at the beginning of this document); the time constants T'_{α} and T'_q are defined below.

By making use of exact results for short times $0 \leq s \leq 2M/(M+1)$ (Lomax et al. 1952), Leishman (2011) shows that:

$$\begin{aligned} T_{\alpha}(M) &= 0.75 \frac{c}{2U} T'_{\alpha} = 0.75 \frac{c}{2Ma_s} T'_{\alpha} = 0.75k_{\alpha}(M)T_I \\ T_q(M) &= 0.75 \frac{c}{2U} T'_q = 0.75 \frac{c}{2Ma_s} T'_q = 0.75k_q(M)T_I \end{aligned} \quad (1.10)$$

where:

$$k_\alpha(M) = [(1 - M) + C_{n\alpha}(M)M^2\beta_M(A_1b_1 + A_2b_2)]^{-1} \quad (1.11a)$$

$$k_q(M) = [(1 - M) + C_{n\alpha}(M)M^2\beta_M(A_1b_1 + A_2b_2)]^{-1} \quad (1.11b)$$

$$T_l = \frac{c}{a_s} \quad (1.11c)$$

where a_s is the speed of sound.

Note that Leishman (2011) recommends the use of the factor 0.75 for $T_\alpha(M)$ and $T_q(M)$ to account for three-dimensional effects not included in piston theory.

For the circulatory component of the aerodynamic force response, the lumped approach can lead to a direct solution of $C_{n\alpha,q}^c(s, M)$. Considering the circulatory part $C_{n\alpha}^c(s, M)$ of Eq. (1.6) for the response to the step in α , it can be written:

$$C_{n\alpha}^c(s, M) = \int_{s_0}^s \frac{C_{n\alpha}(M)}{\beta_M} \phi_\alpha^c \alpha(s) ds \simeq C_{n\alpha}^c(s, M) \Delta\alpha \quad (1.12)$$

$$\text{where } C_{n\alpha}^c(s, M) = \frac{C_{n\alpha}(M)}{\beta_M}$$

By using Eq. (1.4) with $\phi(s, M)$ replaced by ϕ_α^c and $\varepsilon(s)$ by α , Eq. (1.12) rewrites:

$$C_{n\alpha,q}^c(s, M) = C_{n\alpha}^c(s, M) \left[\alpha(s_0) \phi_\alpha^c(s) + \int_{s_0}^s \frac{d\alpha}{d\sigma_s} (\sigma_s) \phi_\alpha^c(s - \sigma_s, M) d\sigma_s \right] = C_{n\alpha}^c(s, M) \alpha_e \quad (1.13)$$

where α_e is an effective angle of attack at $3/4$ -chord accounting for a step variation in α , pitching rate, heave, and velocity (lumped approach). By applying the first of Eq. (1.9), and setting $s_0 = 0$, Eq. (1.13) can be simplified to arrive at an expression for α_e at the n -th time step, (i.e., α_{e_n}):

$$\alpha_{e_n}(s, M) = (\alpha_n - \alpha_0) - X_{1n}(\Delta s) - X_{2n}(\Delta s) \quad (1.14)$$

where the $\int_{s_0}^s [\dots] d\sigma_s$ was numerically integrated. By carrying out the algebra, a recursive expression for X_1 and X_2 can be found:

$$X_{1n} = X_{1n-1} \exp(-b_1 \beta_M^2 \Delta s) + A_1 \exp(-b_1 \beta_M^2 \frac{\Delta s}{2}) \Delta\alpha_n \quad (1.15)$$

$$X_{2n} = X_{2n-1} \exp(-b_2 \beta_M^2 \Delta s) + A_2 \exp(-b_2 \beta_M^2 \frac{\Delta s}{2}) \Delta\alpha_n$$

Note that α_0 was introduced into Eq. (1.14) because α_e is an effective angle of incidence (AOI) and not AOA.

Similar to the above development, the circulatory contribution to $C_{n\alpha,q}^c(s, M)$ from a step change in q can be derived as:

$$C_{nq}^c(s, M) = \frac{C_{n\alpha}^c(s, M)}{2} [q - X_3(\Delta s) - X_4(\Delta s)] \quad (1.16)$$

with

$$X_{3n} = X_{3n-1} \exp(-b_1 \beta_M^2 \Delta s) + A_1 \exp(-b_1 \beta_M^2 \frac{\Delta s}{2}) \Delta q \quad (1.16a)$$

$$X_{4n} = X_{4n-1} \exp(-b_2 \beta_M^2 \Delta s) + A_2 \exp(-b_2 \beta_M^2 \frac{\Delta s}{2}) \Delta q$$

Eqs. (1.16)-(1.16a) are used by González (2014).

However, following the original LBM method, the lumped approach can account for any effect to α , including step changes in q , so Eq. (1.16) is not necessary and is virtually included via Eq. (1.13) and (1.14).

The noncirculatory part cannot be handled via the superposition (lumped approach); therefore, the contribution from step changes in α and q need to be kept separate:

$$C_{n\alpha,q}^{nc}(s, M) = C_{n\alpha}^{nc}(s, M) + C_{nq}^{nc}(s, M) \quad (1.17)$$

Now, using Duhamel's integral (1.4) on the noncirculatory component $C_{n\alpha}^{nc}(s, M)$ [see Eq. (1.17)] with the ϕ_α^{nc} from Eq. (1.9), the following can be arrived at:

$$\begin{aligned} C_{n\alpha}^{nc}(s, M) &= \frac{4T_\alpha(M)}{M} (K_\alpha - K'_\alpha) \\ K'_{\alpha n} &= K'_{\alpha n-1} \exp\left(-\frac{\Delta}{T_\alpha(M)}\right) + (K_{\alpha n} - K_{\alpha n-1}) \exp\left(-\frac{\Delta}{2T_\alpha(M)}\right) \end{aligned} \quad (1.18)$$

Note that in Eq. (1.18), K'_α is the deficiency function for $C_{n\alpha}^{nc}(s, M)$.

For $C_{nq}^{nc}(s, M)$, an analogous procedure leads to:

$$\begin{aligned} C_{nq}^{nc}(s, M) &= -\frac{T_q(M)}{M} (K_{q_n} - K'_{q_n}) \\ K'_{q_n} &= K'_{q_n-1} \exp\left(-\frac{\Delta}{T_q(M)}\right) + (K_{q_n} - K_{q_n-1}) \exp\left(-\frac{\Delta}{2T_q(M)}\right) \end{aligned} \quad (1.19)$$

So finally, the expression for the total normal force under attached conditions C_n^{pot} can be expressed as:

$$\begin{aligned} C_n^{pot} &= C_n^{pot,c} + C_n^{pot,nc} \\ C_n^{pot} &= C_{n\alpha,q}^c(s, M) + C_{n\alpha,q}^{nc}(s, M) = C_{n\alpha}^c(s, M)\alpha_e + \frac{4T_\alpha(M)}{M} (K_{\alpha n} - K'_{\alpha n}) + \frac{T_q(M)}{M} (K_q - K'_q) \end{aligned} \quad (1.20)$$

with

$$\begin{aligned} C_n^{pot,c} &= C_{n\alpha,q}^c(s, M) = C_{n\alpha}^c(s, M)\alpha_e \\ C_n^{pot,nc} &= C_{n\alpha,q}^{nc}(s, M) = \frac{4T_\alpha(M)}{M} (K_\alpha - K'_\alpha) + \frac{T_q(M)}{M} (K_q - K'_q) \end{aligned}$$

1.1.2 Chordwise Force

The chordwise force can be written as in Eq. (1.21) from Leishman (2011):

$$C_c^{pot} = C_n^{pot,c} \tan(\alpha_e + \alpha_0) \quad (1.21)$$

In potential flow, D'Alambert's paradox leads to the absence of drag; therefore, from Eq. (1.3), $C_l \cos \alpha = C_n$ and $C_c = C_l \sin \alpha$, which bring forth Eq. (1.21). Because α_e is a virtual angle of incidence at $3/4$ -chord, we needed to add the α_0 . Because this drag treatment has roots only in the circulatory lift derivation, the noncirculatory part is dropped as shown in Eq. (1.21).

1.1.3 Pitching Moment

Analogous to the normal force treatment, the pitching moment coefficient about the 1/4-chord can be derived via indicial response as shown in Eq. (1.22):

$$\begin{aligned}
 C_{m_{\alpha,q}}(s, M) &= C_{m_{\alpha}}(s, M) + C_{m_q}(s, M) = C_{m_{\alpha}} \alpha + C_{m_q}(s, M) q \\
 C_{m_{\alpha}}(s, M) &= -\frac{1}{M} \phi_{m,\alpha}^{nc} - \frac{C_{n\alpha}(M)}{\beta_M} \phi_{\alpha}^c (\hat{x}_{AC} - 0.25) + C_{m0} \\
 C_{m_q}(s, M) &= -\frac{7}{12M} \phi_{m,q}^{nc} - \frac{C_{n\alpha}(M)}{16\beta_M} \phi_{m,q}^c
 \end{aligned} \tag{1.22}$$

where \hat{x}_{AC} is the aerodynamic center distance from LE in percent chord, C_{m0} (the 2D pitching moment coefficient at 0-lift, positive if nose up) is positive if it causes a pitch up of the airfoil, as seen in Figure 3. Also note that the circulatory component of the pitching moment response to a step change in α is a function of the $C_{n\alpha}^c(s, M)$.

The indicial response can be approximated [see also Eq. (1.9)] as:

$$\phi_{m,q}^{nc} = \exp\left(-\frac{s}{T'_{m,q}}\right) \tag{1.23}$$

Analogous expressions can be found for $\phi_{m,q}^c$ and $\phi_{m,\alpha}^{nc}$, but they are not shown here because further simplified expressions will be derived below. In Eq. (1.23), $T'_{m,q}$ is the Mach-dependent time constant in the expression of $\phi_{m,q}^{nc}$, whose expression can be derived in a similar fashion to those of the constants in Eq. (1.10):

$$T_{m,q}(M) = \frac{c}{2U} T'_{m,q} = \frac{c}{2M\alpha_s} T'_{m,q} = k_{m,q}(M) T_I \tag{1.24}$$

Following Johansen (1999), the circulatory component $C_{m_q}^c(s, M)$ can be written as:

$$C_{m_q}^c(s, M) = -\frac{C_{n\alpha}(M)}{16\beta_M} (q - K_q''') \frac{c}{U} \tag{1.25}$$

where:

$$K_q''' = K_q'''_{n-1} \exp(-b_5 \beta_M^2 \Delta s) + A_5 \Delta q_n \exp\left(-b_5 \beta_M^2 \frac{\Delta s}{2}\right) \tag{1.26}$$

with A_5 and b_5 constants set to 1 and 5, respectively, from experimental results (Leishman 2006).

The noncirculatory component of the pitching moment response to the step change in α , $C_{m_{\alpha}}^{nc}(s, M)$, writes (Leishman and Beddoes 1986; Johansen 1999):

$$C_{m_{\alpha}}^{nc}(s, M) = -\frac{1}{M} \phi_{m,\alpha}^{nc} = -\frac{C_{n\alpha}^{nc}(s, M)}{4} \tag{1.27}$$

which implies

$$\phi_{m,\alpha}^{nc} = \phi_{\alpha}^{nc} \tag{1.28}$$

The other noncirculatory component, $C_{m_q}^{nc}(s, M)$, writes (Leishman 2006):

$$C_{m_q}^{nc}(s, M) = -\frac{7}{12M} \phi_{m,q}^{nc} = -\frac{7k_{m,q}(M)^2 T_I}{12M} (K_q - K_q'') \tag{1.29}$$

with:

$$\begin{aligned}
 k_{m,q}(M) &= \frac{7}{15(1-M) + 1.5C_{n\alpha}(M)A_5b_5\beta_M M^2} \\
 K_q'' &= K_q''_{n-1} \exp\left(-\frac{\Delta t}{k_{m,q}(M)^2 T_I}\right) + (K_{q_n} - K_{q_{n-1}}) \exp\left(-\frac{\Delta t}{2k_{m,q}(M)^2 T_I}\right)
 \end{aligned}$$

where the same procedure was used to arrive at a deficiency function using Duhamel's integral [Eq. (1.4)] and equating the expressions of the $C_{m_{\alpha,q}}(s, M)$ at $s \rightarrow 0$ (Leishman 2006).

Finally, the expression for the total pitching moment at $1/4$ -chord under attached conditions can be expressed as:

$$\begin{aligned}
C_m^{pot} &= C_{m_{\alpha,q}}^c(s, M) + C_{m_{\alpha,q}}^{nc}(s, M) = \\
&C_{m0} - \frac{C_{n\alpha}(M)}{\beta_M} \phi_\alpha^c(\hat{x}_{AC} - 0.25) + \\
&-\frac{C_{n\alpha}(M)}{16\beta_M} (q - K_q''') \frac{c}{U} + \\
&-\frac{T_\alpha(M)}{M} (K_\alpha - K'_\alpha) + \\
&-\frac{7k_{m,q}(M)^2 T_I}{12M} (K_q - K_q'')
\end{aligned} \tag{1.30}$$

Note that the pitching moment treatment is slightly different from what is in AeroDyn v.13 and Damiani (2011) and it is more in line with Leishman (2006) and Johansen (1999). If Minnema's (1998) method is used, then the $C_{m_q}^{nc}(s, M)$ [last term in Eq. (1.30)] is to be replaced by:

$$C_{m_q}^{nc}(s, M) = -\frac{7}{12M} \phi_{m,q}^{nc} = -\frac{C_{n_q}^{nc}(s, M)}{4} - \frac{k_\alpha(M)^2 T_I}{3M} (K_q - K_q'') \tag{1.31}$$

1.2 TE Flow Separation

The basis of this dynamic system is Kirchoff's theory, which can be expressed as follows (Leishman 2006):

$$\begin{aligned}
C_n(\alpha, f, s, M) &= C_{n\alpha}^c(s, M) (\alpha - \alpha_0) \left(\frac{1+\sqrt{f}}{2} \right)^2 \\
C_c(\alpha, f, s, M) &= \eta_e C_{n\alpha}^c(s, M) (\alpha - \alpha_0) \sqrt{f} \tan(\alpha)
\end{aligned} \tag{1.32}$$

where f is the separation point distance from LE in percent chord and η_e the recovery factor $\simeq [0.85 - 0.95]$ to account for viscous effects at limited or no separation on C_c .

If the airfoil's C_l , C_d , and C_m characteristics are known, then Eq. 1.32 may be solved for f . Leishman (2011) suggests the use of best-fit curves obtained from static measurements on airfoils, of the type:

$$f = \begin{cases} 1 - 0.3 \exp\left(\frac{\alpha - \alpha_1}{S_1}\right), & \text{if } \alpha_0 \leq \alpha \leq \alpha_1 \\ 1 - 0.3 \exp\left(\frac{\alpha_2 - \alpha}{S_3}\right), & \text{if } \alpha_2 \leq \alpha < \alpha_0 \\ 0.04 + 0.66 \exp\left(\frac{\alpha_1 - \alpha}{S_2}\right), & \text{if } \alpha > \alpha_1 \\ 0.04 + 0.66 \exp\left(\frac{\alpha - \alpha_2}{S_4}\right), & \text{if } \alpha < \alpha_2 \end{cases} \tag{1.33}$$

S_1 - S_2 (and the analogous S_3 - S_4 for $\alpha < \alpha_0$) are best-fit constants that define the abruptness of the static stall. α_1 is the angle of attack at $f=0.7$ (approximately the stall angle), for $\alpha \geq \alpha_0$, whereas α_2 is the angle of attack at $f=0.7$ for $\alpha < \alpha_0$.

Accounting for unsteady conditions, the TE separation point gets modified because of temporal effects on airfoil pressure distribution and boundary layer response. LE separation occurs when a critical pressure at the leading edge, corresponding to a critical value of the normal force C_{n1} , is reached.

1.2.1 Normal Force

The circulatory normal force needs to be modified to account for the lagged boundary layer response. To arrive at a new expression for C_n , we start by accounting for the separation point location under unsteady conditions, which can be calculated starting from an effective AOI, α_f :

$$\alpha_f = \frac{C'_n}{C_{n\alpha}^c(s, M)} + \alpha_0 \quad (1.34)$$

where an effective C'_n is used and calculated as in Eq. (1.35):

$$\begin{aligned} C'_n &= C_n^{pot} - D_p \\ D_{p_n} &= D_{p_{n-1}} \exp\left(-\frac{\Delta s}{T_p}\right) + (C_n^{pot} - C_{n-1}^{pot}) \exp\left(-\frac{\Delta s}{2T_p}\right) \end{aligned} \quad (1.35)$$

Note T_p is the boundary-layer, LE pressure gradient time constant in the expression of D_p , which should be tuned based on airfoil experimental data. Johansen (1999) employs two time constants, $T_{p\alpha}$ and T_{pq} , as the C'_n is separated into two contributions, one from α and from q .

Given the new C'_n , a new formulation can be obtained for f (i.e., f''), which accounts for delays in the boundary layer and will be used via Kirchhoff's treatment to arrive at the new C_n :

$$\begin{aligned} f'' &= f' - D_f \\ D_{f_n} &= D_{f_{n-1}} \exp\left(-\frac{\Delta s}{T_f}\right) + (f'_n - f'_{n-1}) \exp\left(-\frac{\Delta s}{2T_f}\right) \end{aligned} \quad (1.36)$$

where f' is the separation point distance from LE in percent chord under unsteady conditions that can be obtained from the best-fit in Eq. (1.33) replacing α with α_f .

Alternatively, f' can be derived from a direct lookup table of static airfoil data reversing Eq. (1.32). In fact, two values of f' could be calculated: one for C_n (f'_n) and one for C_c (f'_c).

Also note that T_f is a constant dependent on Mach, Re , and airfoil shape; it is used in the expression of D_f and f'' and it is associated with the motion of the separation point along the suction surface of the airfoil. T_f gets modified via multipliers (σ_1) that depend on the phase of the separation or reattachment as discussed later; here it suffices noting that T_f can be written as a modified version of the initial value T_{f0} :

$$T_f = T_{f0}/\sigma_1 \quad (1.37)$$

Finally, the normal force coefficient C_n^{fs} , after accounting for separated flow from the TE, becomes:

$$C_n^{fs} = C_{n\alpha,q}^{nc}(s, M) + C_{n\alpha,q}^c(s, M) \left(\frac{1 + \sqrt{f''}}{2}\right)^2 = C_{n\alpha,q}^{nc}(s, M) + C_{n\alpha}^c(s, M) \alpha_e \left(\frac{1 + \sqrt{f''}}{2}\right)^2 \quad (1.38)$$

Note that González (2014) and Sheng, Galbraith, and Coton (2007) propose the corrective factor to be:

$$C_n^{fs} = C_{n\alpha,q}^{nc}(s, M) + C_{n\alpha}^c(s, M) \alpha_e \left(\frac{1 + 2\sqrt{f''}}{3}\right)^2 + C_{n_q}^c(s, M) \quad (1.39)$$

The last term in Eq. (1.39) is calculated via Eq. (1.16). The corrective factor $\left(\frac{1 + 2\sqrt{f''}}{3}\right)^2$ was proposed to account for lower values of C_n when $f=0$ that were seen from experimental data.

1.2.2 Chordwise Force

The along-chord force coefficient analogously becomes:

$$C_c^{fs} = C_c^{pot} \eta_e \left(\sqrt{f''} - 0.2 \right) \quad (1.40)$$

where the 0.2 factor is used by González (2014) to modify $\sqrt{f''}$ to account for negative values seen at $f=0$.

1.2.3 Pitching Moment

Now turning to the pitching moment, the contribution caused by unsteady separated flow is on the circulatory component alone. Leishman (2011) suggests using this formulation that modified C_m^{pot} for the $C_{m\alpha}^c(s, M)$ component:

$$C_m^{fs} = C_{m0} - C_{n\alpha,q}^c(s, M)(\hat{x}_{cp} - 0.25) + C_{m_q}^c(s, M) + C_{m\alpha}^{nc}(s, M) + C_{m_q}^{nc}(s, M) \quad (1.41)$$

where \hat{x}_{cp} is the center-of-pressure distance from LE in percent chord and can be approximated by (Leishman 2011):

$$\hat{x}_{cp} = k_0 + k_1 (1 - f'') + k_2 \sin(\pi f''^{k_3}) \quad (1.42)$$

where $k_0=0.25-\hat{x}_{AC}$, and the k_1-k_3 constants are calculated via best fits of experimental data. Other expressions could be used to perform the best fit of \hat{x}_{cp} versus f from static C_m airfoil data.

Minnema (1998) suggests a different approach where an effective lagged AOI is calculated as follows:

$$\begin{aligned} \alpha'_f &= \alpha_f - D_{\alpha f} \\ D_{\alpha f_n} &= D_{\alpha f_{n-1}} \exp\left(-\frac{\Delta s}{0.1T_f}\right) + (\alpha_{f_n} - \alpha_{f_{n-1}}) \exp\left(-\frac{\Delta s}{2*0.1T_f}\right) \end{aligned} \quad (1.43)$$

Note that T_f is factored by 0.1 following Minnema (1998) validation results. Then the new AOI is used to derive the contribution to the circulatory component of the pitching moment, which is extracted from a lookup table of static coefficients C_m versus α .

$$C_m^{fs} = C_m(\alpha'_f) + C_{m_q}^c(s, M) + C_{m\alpha}^{nc}(s, M) + C_{m_q}^{nc}(s, M) \quad (1.44)$$

The method proposed by González (2014) [see Eq. (1.45)] uses a value of f' ($=f'_m$) extracted from a static data table where it is assumed that $C_m - C_{m0} = f_m C_n$ (loosely correlating f to \hat{x}_{cp}). The angle used for interpolation of the lookup table is α_f . To resolve the contribution to C_m from the unsteady TE separation, this method should then use the full C_n^{fs} from Eq. (1.39) and the lagged f'_m calculated from f'_m and Eq. (1.36), replacing f' with f'_m . However, for the current implementation of the UAM, there is no further lagging of the f'_m quantity. This may change in future versions of UAM.

$$C_m^{fs} = C_{m0} + C_n^{fs} f'_m + C_{m_q}^c(s, M) + C_{m\alpha}^{nc}(s, M) + C_{m_q}^{nc}(s, M) \quad (1.45)$$

In this case, the two treatments (Minnema 1998; González 2014) seem somewhat equivalent, with the exception that González (2014) proposes 21 (7 for each f'' related to C_n , C_c , and C_m) different multipliers for T_f depending on the state of the airfoil aerodynamics (e.g., increasing AOA and above a critical C_{n1} , increasing AOA and below a critical C_{n1}).

1.3 Dynamic Stall

1.3.1 Normal Force

During DS, there is shear layer roll up at the LE with associated vortex formation, and vortex travel over the upper surface of the airfoil that will be subsequently shed in the wake. The main condition to be met for the shear layer roll up is:

$$\begin{aligned} C_n' &> C_{n1} && \text{for } \alpha \geq \alpha_0 \\ C_n' &< C_{n2} && \text{for } \alpha < \alpha_0 \end{aligned} \quad (1.46)$$

The normal force coefficient contribution from the additional lift associated with the low-pressure LE vortex can be written as (Leishman 2011):

$$C_{n,n}^v = C_{n,n-1}^v \exp\left(-\frac{\Delta s}{T_V}\right) + (C_{Vn} - C_{Vn-1}) \exp\left(-\frac{\Delta s}{2T_V}\right) \quad (1.47)$$

T_V is the time constant associated with the vortex lift decay process and it depends on Re , M , and airfoil type. Note that the C_n^v contribution is not allowed to have a sign opposite to that of C_n^{fs} .

T_V gets modified via a multiplier σ_3 to account for various stages of the process, as discussed later, but here it suffices to say that:

$$T_V = T_{V0}/\sigma_3 \quad (1.48)$$

C_V represents the contribution to the normal force coefficient due to accumulated vorticity in the LE vortex. C_V is modeled proportionally to the difference between the attached and separated circulatory contributions to C_n :

$$C_V = C_{n\alpha,q}^c(s, M) - C_{n\alpha,q}^c(s, M) \left(\frac{1 + \sqrt{f''}}{2}\right)^2 = C_{n\alpha}^c(s, M) \alpha_e \left(1 - \frac{1 + \sqrt{f''}}{2}\right)^2 \quad (1.49)$$

If the method proposed by González (2014) is used, then C_V can be written as:

$$C_V = C_{n\alpha}^c(s, M) \alpha_e \left(1 - \frac{1 + 2\sqrt{f''}}{3}\right)^2 \quad (1.50)$$

The position of the LE vortex along the chordwise direction is tracked via a nondimensional time variable, τ_V , defined in Eq. (1.51):

$$\tau_V = t \frac{2U}{c} \quad (1.51)$$

If $\tau_V=0$, the vortex is at the LE; if $\tau_V=T_{VL}$, the vortex is at the TE.

If $\tau_V > T_{VL}$ and if α_f is not moving away from stall (i.e., $[(\alpha_f - \alpha_0) * (\alpha_{fn} - \alpha_{fn-1})] > 0$), then the vorticity is no longer allowed to accumulate, in which case Eq. (1.47) can be rewritten as:

$$\begin{aligned} C_{n,n}^v &= C_{n,n-1}^v \exp\left(-\frac{\Delta s}{T_{V0}/\sigma_3}\right) \\ \text{with } \sigma_3 &= 2 \end{aligned} \quad (1.52)$$

where the decay of the normal force (due to vorticity at the LE) is accelerated at twice the original rate and no further accretion of vorticity is allowed. Eq. (1.52) should also be used when conditions in Eq. (1.46) are not met. Note that T_{VL} represents the time constant associated with the vortex advection process; it represents the nondimensional time in semichords needed for a vortex to travel from LE to TE; it is used in the expression of C_n^v ; it depends on Re , M (weakly), and airfoil. Value's range = [6; 13].

Finally, the total normal force can be written as:

$$C_n = C_n^{fs} + C_n^v = C_{n\alpha}^c(s, M) \alpha_e \left(\frac{1 + \sqrt{f''}}{2}\right)^2 + C_{n\alpha,q}^{nc}(s, M) + C_n^v \quad (1.53)$$

Again, if González's (2014) method is used, then the correction factor for the separated flow treatment is slightly modified as in Eq. (1.50), for example:

$$C_n = C_n^{fs} + C_n^v = C_{n\alpha}^c(s, M) \alpha_e \left(\frac{1 + 2\sqrt{f''}}{3} \right)^2 + C_{n\alpha,q}^{nc}(s, M) + C_n^v \quad (1.53b)$$

Note that multiple vortices can be shed at a given shedding frequency corresponding to:

$$T_{sh} = 2 \frac{1 - f''}{St_{sh}} \quad (1.54)$$

Therefore, τ_v is reset to 0 if $\tau_v = T_{VL} + T_{sh}$.

1.3.2 Chordwise Force

The along-chord force coefficient gets modified by the presence of the LE vortex as in Pierce (1996):

$$C_c = C_c^{fs} + C_n^v \tan(\alpha_e) \left(1 - \frac{\tau_v}{T_{VL}} \right) \quad (1.55)$$

Note that in the current release of UA, the $\tan(\alpha_e) \simeq \alpha_e$ approximation is made. This may be changed after testing in future releases.

González (2014) does not contain the vortex contribution to C_c based on experimental validation:

$$C_c = C_c^{fs} \quad (1.55b)$$

The original Leishman and Beddoes (1989) model had C_c written as:

$$C_c = \begin{cases} \eta_e C_c^{pot} \sqrt{f''} \sin(\alpha_e + \alpha_0) & , C'_n \leq C_{n1} \\ \hat{k}_1 + C_c^{pot} \sqrt{f''} f''^{\hat{k}_2} \sin(\alpha_e + \alpha_0) & , C'_n > C_{n1} \end{cases} \quad (1.56a)$$

$$\text{with : } \hat{k}_2 = 2(C'_n - C_{n1}) + f'' - f \quad (1.56b)$$

where \hat{k}_1 is a constant required to fit the C_c curve under static conditions for 2D airfoils.

1.3.3 Pitching Moment

Leishman (2011) offers a form for the \hat{x}_{cp}^v , which is the center-of-pressure distance from the $1/4$ -chord, in percent chord, during the LE vortex advection process:

$$C_m^v = -\hat{x}_{cp}^v C_n^v \\ \hat{x}_{cp}^v(\tau_v) = \bar{\bar{x}}_{cp} \left(1 - \cos\left(\frac{\pi\tau_v}{T_{VL}}\right) \right) \quad (1.57)$$

where $\bar{\bar{x}}_{cp}$ is a constant in the expression of \hat{x}_{cp}^v , usually equal to 0.2.

Finally, the expression for the total pitching moment can be written as:

$$C_m = C_{m0} - C_{n\alpha,q}^c(s, M)(\hat{x}_{cp} - 0.25) + C_{m_q}^c(s, M) + C_{m\alpha}^{nc}(s, M) + C_{m_q}^{nc}(s, M) + C_m^v \quad (1.58)$$

If Minnema's (1998) approach is used, then Eq. (1.58) can be rewritten as:

$$C_m = C_m(\alpha_f') + C_{m_q}^c(s, M) + C_{m\alpha}^{nc}(s, M) + C_{m_q}^{nc}(s, M) + C_m^v \quad (1.59)$$

and if González's (2014) treatment is used, the total moment becomes:

$$C_m = C_n f_m'' + C_{m_q}^c(s, M) + C_{m\alpha}^{nc}(s, M) + C_{m_q}^{nc}(s, M) + C_m^v \quad (1.60)$$

2 Inputs, Outputs, Parameters, States, and Implementation of UA

The UA implementation loosely follows the FAST modularization framework. This includes key interface routines for module initialization (UA_Init), updating the module's states (UA_UpdateStates), and generating module outputs (UA_CalcOutput). Because the UAM module does not communicate directly with the FAST glue code, we have taken some liberties with regard to the arguments to these interface routines. Additionally, the typical framework data structures for inputs (u) and outputs (y) have been modified to allow for a more intuitive integration into either a BEMT/dynamic blade element momentum theory (DBEMT) algorithm or the generalized dynamic wake (GDW) algorithm. In the following sections, the inputs/states/parameters are listed, then each interface routine will be discussed, and any deviations from the FAST framework will be highlighted.

To provide the context for the UAM, the flow diagram from AeroDyn to UA is shown in Figure 4.

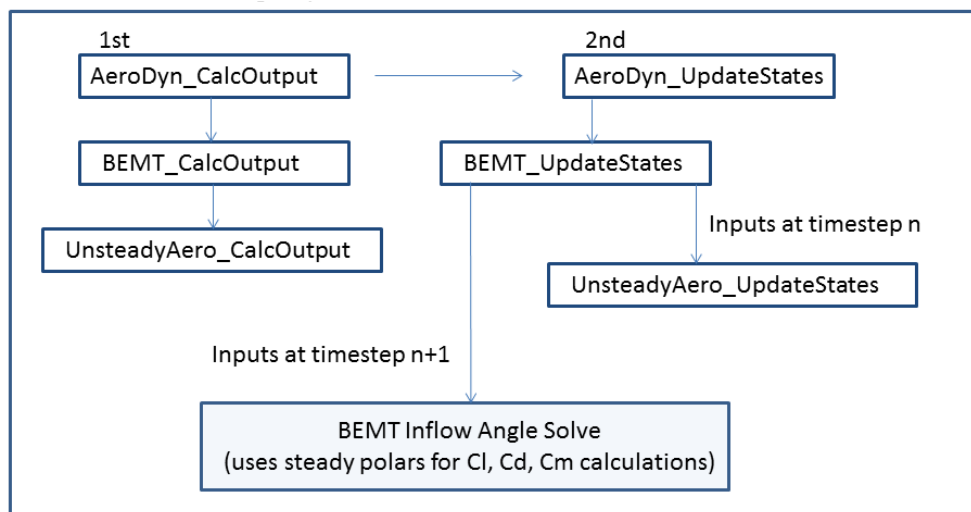


Figure 4. Block diagram showing the order of the calls to the subroutines (AeroDyn_CalcOutput happens first, AeroDyn_UpdateStates happens second) and the overall organization from the parent module AeroDyn to UA

2.1 Init_Inputs

In addition to the standard variables common to all modules (e.g., *NumOuts*, i.e., number of output channels), the *Init_Inputs* to the UA are:

- Δt – time step
- a_s – speed of sound
- *UAmo*d – switch to select handling of options and possible methods in the UA treatment
- *flookup* – logical flag to indicate whether a lookup (True) or an interpolation of the airfoil data tables (False) is used to retrieve the values for f
- *nNodesPerBlade* – number of nodes per blade (used for array allocation)
- *NumBlades* – number of blades (used for array allocation)
- c – airfoil chord at each blade station for each blade.

2.2 Inputs u

The inputs to the UA are:

- α
- U
- Re .

Note: these are for a given node (within a given blade).

2.3 Outputs y

The outputs from the UA are:

- C_n
- C_c
- C_m
- C_l
- C_d (this includes the viscous shear component C_{d0}).

Note: these are for a given node (within a given blade).

2.4 States x_d

The states for the UA are:

Discrete states:

- $\alpha_{,-1}$ – previous time-step value of α
- $\alpha_{LP,-1}$ – previous time-step value of low-pass-filtered α
- $\alpha_{f,-1}$ – previous time-step value of α_f
- $q_{,-1}$ – previous time-step value of q
- $q_{LP,-1}$ – previous time-step value of low-pass-filtered q
- $K_{\alpha LP,-1}$ – previous time-step value of low-pass-filtered K_α
- $K_{q LP,-1}$ – previous time-step value of low-pass-filtered K_q
- $X_{1,-1}$ – previous time-step value of X_1
- $X_{2,-1}$ – previous time-step value of X_2
- $X_{3,-1}$ – previous time-step value of X_3
- $X_{4,-1}$ – previous time-step value of X_4
- $K'_{\alpha,-1}$ – previous time-step value of K'_α
- $K'_{q,-1}$ – previous time-step value of K'_q
- $K''_{q,-1}$ – previous time-step value of K''_q
- $K'''_{q,-1}$ – previous time-step value of K'''_q
- $D_{p,-1}$ – previous time-step value of D_p

- $D_{f,-1}$ – previous time-step value of D_f
- $D_{f_c,-1}$ – previous time-step value of D_{f_c} (D_{f_c} is the deficiency function for f'_c analogous to D_f)
- $C_n^{pot,-1}$ – previous time-step value of C_n^{pot}
- $f'_{,-1}$ – previous time-step value of f'
- $f'_{c,-1}$ – previous time-step value of f'_c
- $f''_{,-1}$ – previous time-step value of f''
- $f''_{c,-1}$ – previous time-step value of f''_c (f''_c is the lagged version of f'_c)
- τ_V – time variable that tracks the travel of the LE vortex over the airfoil suction surface. It is made dimensionless via the semichord: $\tau_V = t * 2U/c$. If less than $2T_{VL}$, it renders the logical flag $VRTX=True$; if less than T_{VL} , then the vortex is still on the airfoil
- $\tau_{V,-1}$ – previous time-step value of τ_V
- $C_n^v_{,-1}$ – previous time-step value of C_n^v
- $C_V_{,-1}$ – previous time-step value of C_V
- $D_{\alpha f,-1}$ – previous time-step value of $D_{\alpha f}$

The FAST 8 framework does not allow logical or discontinuous variables within states. For this reason, the following are declared as either *Other States* or *miscVars* (other local variables (not saved between calls to *UpdateStates* and *CalcOutputs* and when backing up in time)).

Other states:

- σ_1 – generic multiplier for T_f
- σ_3 – generic multiplier for T_V

miscVars:

- *iBlade* – blade index
- *jBladeNode* – blade node index
- *TESF* – trailing-edge separation flag
- *LESF* – leading-edge separation flag
- *VRTX* – vortex advection flag
- *FirstPass* - flag indicating first time step

Note that, in contrast to inputs and outputs, the states must be tracked by the UA module; therefore, they are a 2-D array (per blade, per node).

2.5 Parameters p

The parameters for the UA are:

- Δt – time step
- c – chord length
- *UAmo*d – switch to select handling of options and possible methods in the UA treatment
- a_s – speed of sound

- *flookup* – logical flag to indicate whether a lookup (True) or an interpolation of the airfoil data tables (False) is used to retrieve the values for *f*
- ζ_{LP} – low-pass-filter frequency cutoff (–3 dB)
- *nNodesPerBlade* – number of nodes per blade
- *NumBlades* – number of blades

An airfoil data structure (*AFIParams*) is passed directly to the UAM framework routines and is indexed to the airfoil of interest. *AFIParams* contains airfoil-specific quantities, i.e., parameters and constants for the UA, although it is not formally a parameter of the FAST 8 framework:

- $\alpha_0, \alpha_1, \alpha_2, C_{n\alpha}(M), C_{n1}, C_{n2}, \eta_e, C_{d0}, C_{m0}, \bar{x}_{cp}, St_{sh}$
- $A_1, b_1, A_2, b_2, A_5, b_5$
- S_1, S_2, S_3, S_4
- T_p (fairly independent of airfoil type)
- T_{f0}, T_{V0}, T_{VL}
- k_0, k_1, k_2, k_3
- \hat{k}_1 .

These parameters were introduced in this manual and their meanings are provided in the list of symbols at the beginning of the document.

2.6 UA Implementation

2.6.1 UA_Init Routine

This routine allocates the module’s data structures and sets the nontime-varying parameters (copies them from the initialization input data section).

2.6.2 UA_UpdateStates Routine

The typical list of arguments to *UA_UpdateStates* gets augmented to pass indices to the blade and blade node of interest and the structure *AFIParams*, which contains the airfoil data.

The model is of the parsimonious, open-loop, Kelvin-chain kind. Outputs of each subsystem serve as inputs to the next subsystem. There are no differential equations to solve. There is no solver per se; for this reason states are discrete states only (see Section 2.4 for other states).

2.6.2.1 UAmod Logical Flags

The options implemented in the code are selected via the *UAmod* switch and *flookup* flag:

- *UAmod*=1: closest model to the original Leishman-Beddoes formulation
- *UAmod*=2: modifications to the original model and simplifications following González (2014)
- *UAmod*=3: modifications to the original model and simplifications following Pierce (1996) and Minnema (1998)
- *flookup*=True: Eq. (1.33) gets replaced by lookup values for f'_n, f'_c . Note that if *UAmod*=2 or 3, the flag is automatically set to True.

In what follows, the modifications to the algorithm for *UAmod*=2 or 3 are given with respect to the sequence of equations used for *UAmod*=1.

If $U_{Amod}=2$, then:

- Replace Eq. (1.58) with Eq. (1.60)
- Replace Eq. (1.56) with Eq. (1.55b)
- Replace Eq. (1.53) with Eq. (1.53b)
- Replace Eq. (1.49) with Eq. (1.50)
- Replace Eq. (1.41) with Eq. (1.45)
- Replace Eq. (1.38) with Eq. (1.39)
- Add Eq. (1.16) to $C_{n\alpha,q}^c(s,M)$ Eq. (1.13).

If $U_{Amod}=3$, then:

- Replace Eq. (1.56) with Eq. (1.55)
- Replace Eq. (1.58) with Eq. (1.59)
- Replace Eq. (1.41) with Eq. (1.43)-(1.44)
- Modify Eq. (1.30) with Eq. (1.31).

2.6.2.2 Update Discrete States

For a given set of inputs, (u), and at the current step in time, (t), the Kelvin chain is performed through the following equations:

- Eq. (1.11c)
- Eq. (1.5b)
- Eq. (1.7)-(1.8)
- Eq. (1.11a) (calculated solely at first time step)
- Eq. (1.11b) (calculated solely at first time step)
- Eq. (1.10)
- Eq. (1.37)
- Eq. (1.48)
- Eq. (1.18)
- Eq. (1.19)
- Eq. (1.17)
- Eq. (1.15)
- Eq. (1.14)
- Eq. (1.13)
- Eq. (1.26)
- Eq. (1.25)
- Eq. (1.20)
- Eq. (1.29)
- Eq. (1.21)
- Eq. (1.35)
- Eq. (1.34)
- Eq. (1.33)

- Eq. (1.36)
- Eq. (1.38) [or Eq. (1.39)]
- Eq. (1.49) [or Eq. (1.50)]
- Eq. (1.47) [or Eq. (1.52)].

2.6.2.3 Update Other States

- If $C'_n > C_{n1}$ ($C'_n < C_{n2}$ for $\alpha < \alpha_0$), Then:
 $LESF=True$: this means LE separation can occur
 Else
 $LESF=False$: this means reattachment can occur
- If $f''_t < f''_{t-1}$, Then:
 $TESF=True$: this means TE separation is in progress
 Else
 $TESF=False$: this means TE reattachment is in progress
- If $0 < \tau_V \leq 2T_{VL}$, Then:
 $VRTX=True$: this means vortex advection is in progress
 Else
 $VRTX=False$: this means vortex is in wake
- If $\tau_V \geq 1 + \frac{T_{sh}}{T_{VL}}$ and $LESF=True$, Then:
 τ_V is reset to 0.

2.6.2.3.1 T_f modifications

The following conditional statements operate on a multiplier σ_1 that affects T_f , i.e., the actual T_f is given by Eq. (1.37):

$$T_f = T_{f0}/\sigma_1 \quad (1.37 \text{ revisited})$$

where T_{f0} is the initial value of T_f ; $\sigma_1 = 1$ (initialization default value); and $\Delta_{\alpha 0} = \alpha - \alpha_0$

IF $TESF=True$, THEN: (separation)

If $K_\alpha \Delta_{\alpha 0} < 0$, Then: $\sigma_1 = 2$ (accelerate separation point movement)

Else If $LESF=False$, Then: $\sigma_1 = 1$ (default value, LE separation can occur)

Else If $f''_{n-1} \leq 0.7$, Then: $\sigma_1 = 2$ (accelerate separation point movement if separation is occurring)

Else $\sigma_1 = 1.75$ (accelerate separation point movement)

ELSE: (reattachment, this means $TESF=False$)

If $LESF = False$, Then: $\sigma_1 = 0.5$ (default: slow down reattachment)

If $VRTX=True$ and $0 \leq \tau_V \leq T_{VL}$, Then: $\sigma_1 = 0.25$ - No flow reattachment if vortex shedding is in progress

If $K_\alpha \Delta_{\alpha 0} > 0$, Then: $\sigma_1 = 0.75$.

Note the last three conditional statements are separate "ifs."

Although this logic was tested and proved to be effective, the current version of UA uses a simpler version.

2.6.2.3.2 T_V modifications

For T_V , an analogous set of conditions is used to set the proper value of the time constant depending on subsystem stages:

$\sigma_3=1$ (initialization default value)

If $T_{VL} \leq \tau_V \leq 2T_{VL}$, Then

$\sigma_3=3$ (postshedding)
 If $TESF=False$, then:
 $\sigma_3=4$ (accelerate vortex lift decay)
 If $VRTX=True$ and $0 \leq \tau_V \leq T_{VL}$, then:
 If $K_\alpha \Delta_{\alpha 0} < 0$, then $\sigma_3=2$ (accelerate vortex lift decay)
 else $\sigma_3=1$ (default)
 Else if $K_\alpha \Delta_{\alpha 0} < 0$, then: $\sigma_3=4$ (vortex lift must decay fast)
 If $TESF=False$ and $K_q \Delta_{\alpha 0} < 0$, then: $\sigma_3=1$ (default).

2.6.2.3.3 Update ‘previous time step’ states

After the states are updated to the next time step (t+1) values, the current values at time step, t, are stored into the (t-1) states.

2.6.3 UA_CalcOutput

This routine determines the outputs, C_n , C_c (and the transformed versions, C_l and C_d), and C_m given the inputs of U , α , and Re (currently unused), for a given blade element. Because the routine only generates outputs for a specific blade element, the FAST framework arguments are augmented to include indices to the blade and blade node of interest. The routine uses the same Kelvin chain as in `UA_UpdateStates`; however, the state variables themselves are not updated during these calculations.

For the first time step, outputs are determined by static lookup tables.

The equations implemented in this routine are the same as in Section 2.6.2.2, plus the following:

- Eq. (1.53)
- Eq. (1.55)
- Eq. (1.2)
- Eq. (1.58).

Bibliography

- Damiani, R. 2011. *Algorithmic Outline of Unsteady Aerodynamics (AeroDyn) Modules*. Final Report WE-201103. NREL Subcontract No. AFT-1-11326-01 under Prime Contract No. DE-AC36-08GO28308. Available upon request from NREL. Arvada, CO: RRD Engineering, LLC.
- . 2016, forthcoming. *The Dynamic Blade Element Momentum Theory For FAST 8*. Technical Report. In Review. Golden, CO: National Renewable Energy Laboratory (NREL).
- González, A. 2014. *DYSTOOL Stability Aerodynamic Tool for 2D Airfoil Based on the Beddoes-Leishman Model*. Informe IN-523/069-en. Wind Energy Department – Fundación CENER-CIEMAT. Avenida Ciudad de la Innovación, 7 - 31621-Sarriguren (Navarra) Spain: CENER.
- Gupta, S., and J. G. Leishman. 2006. “Dynamic Stall Modeling of the S809 Airfoil and Comparison with Experiments”. *Wind Energy* 9 (6): 521–547.
- Johansen, J. 1999. *Unsteady Airfoil Flows with Application to Aeroelastic Stability*. Report Risø-R-1116(EN). 98 pages. Roskilde, Denmark: Risø National Laboratory.
- Jonkman, J. 2013. “New Modularization Framework for the FAST Wind Turbine CAE Tool”. In *Proceedings of the 51st AIAA Aerospace Sciences Meeting*. Dallas, TX: AIAA.
- Leishman, J. G. 2006. *Principles of Helicopter Aerodynamics*. 2nd. 826 p. New York, NY: Cambridge University Press.
- . 2011. *Final Report: Assessment of ‘AeroDyn’ Theory Basis Including Unsteady Aerodynamics Modules*. NREL Subcontractor Report LFC-1-11303-01. Prime Contract No. DE-AC36-08GO28308.
- Leishman, J. G., and T. S. Beddoes. 1986. “A General Model for Airfoil Unsteady Behavior and Dynamic Stall Using the Indicical Method”. In *Proceedings of the 42nd Annual Forum of the American Helicopter Society*, 243–266. Washington, D.C.: American Helicopter Society.
- . 1989. “A Semi-Empirical Model for Dynamic Stall”. *J. of the American Helicopter Society* 34 (3): 3–17.
- Lomax, H., et al. 1952. *Two and Three Dimensional Unsteady Lift Problems in High Speed Flight*. Technical Report 1077. NACA.
- Minnema, J. E. 1998. *Pitching Moment Predictions on Wind Turbine Blades Using the Beddoes-Leishman Model for Unsteady Aerodynamics and Dynamic Stall*. MA thesis, The University of Utah.
- Pierce, K. G. 1996. *Wind Turbine Load Prediction Using the Beddoes-Leishman Model for Unsteady Aerodynamics and Dynamic Stall*. MA thesis, The University of Utah.
- Pierce, K. G., and A. C. Hansen. 1995. “Prediction of Wind Turbine Rotor Loads Using the Beddoes-Leishman Model for Dynamic Stall”. *J. of Solar Energy Engineering* 117:200–204.
- Sheng, W., R. A. Galbraith, and F. N. Coton. 2007. “A Modified Dynamic Stall Model for Low Mach Numbers”. In *45th AIAA Aerospace Sciences Meeting and Exhibit*.